

Dynamics of micrometer- sized particles in a separated flow over broad crested weir of sharp corners and weir with practical profile

M.I. Attia

Water and Water Structure Eng. Dept., Faculty of Eng., Zagazig University, Zagazig Egypt
e-mail: Melshawi@yahoo.com

This paper presents on experimental investigation of the dynamics of micrometer- sized particles and flow separation over broad crested weir of sharp corners and weir with practical profile. Particles in diameter range from 10 to 100 μm were suspended in a water flow and the particle motion over a broad crested weir of sharp corners was measured by a Laser- Doppler Anemometry (LDA), in a horizontal channel of constant width. Thus, the local integral flow quantities, i.e. the mean and turbulent velocity data could be measured precisely. In the experiments, monodispersed particle size distributions were used to exclude particle size related information ambiguity, known as triggering or size bias. The aim of this investigation is to study the effect of dynamics of micrometer sized particles on the turbulence intensities and mean velocities, and to determine the differences in turbulent flow field quantities over the weir with practical profile and broad crested weir of sharp corners. Flow describing quantities like mean and turbulent velocities, and dividing streamlines of the separation zones were measured by LDA. The results of this investigation show, qualitatively the difference in time averaged particle dynamics for selected particle sizes over a broad crested weir of sharp corners flow. The experiments show the changes in the particle velocity field when compared with the velocity field of the continuous phase, deduced from 10 μm particles. Additionally, the results imply the strong influences of different particle sizes on flow data measurement when size effects are not taken into account with particle- related optical measuring techniques.

يهدف هذا البحث إلى دراسة معملياً لديناميكية الحبيبات المتناهية الصغر ذات الأقطار المختلفة في مناطق السريران العالية الاضطراب فوق الهدار العريض الحاد العتب والهدار ذو المقطع العملي وذلك باستخدام جهاز الليزر (LDA) في القنوات المستطيلة المقطع المفتوحة الأفقية ثابتة العرض. ولهذا الغرض أجريت الدراسة المعملياً للجريان ذات أقطار مختلفة من 10 إلى 100 ميكرون (μm) للحبيبات المعلقة المتناهية الصغر. وتم قياس كثافات الاضطراب والسرعات في اتجاه السريران (spanwise) واتجاه عمق المياه (depthwise) وذلك للجريان المضطرب ذات الحبيبات المعلقة الدقيقة الأقطار. ولدراسة دقيقة لخصائص السريران تم قياس المتغيرات المختلفة للسريران عند قطاعات عرضية مختلفة خلف الهدار. ومن نتائج البحث لهذه الدراسة فقد وضحت ديناميكية السريران ذات الحبيبات الدقيقة المعلقة في المناطق العالية الاضطراب فوق الهدار العريض الحاد الأركان كذلك تم أعداد منحنيات لابعدية لكثافات الاضطراب والسرعات للجريان ذات الحبيبات الدقيقة المختلفة الأقطار. ومن نتائج الدراسة وجد ان سرعة الجريان ذات الحبيبات الكبيرة أكبر من سرعة الجريان ذات الحبيبات الصغيرة وذلك في القطاعات القريبة من الهدار وتذبذب السرعات للجريان ذات السرعات للجريان ذات الحبيبات الكبيرة أقل من السرعات للجريان ذات الحبيبات الصغيرة. وقد تبين أن أبعاد المنطقة العالية الاضطراب (recirculation zone) يقل بزيادة حجم الحبيبات وهذا يرجع إلى نقص السرعات العمودية على اتجاه السريران (Counter streamwise) في هذه المنطقة.

Keywords: Broad-crested weir, Sediment transportation, Turbulent velocities over a broad-crested weir, weir with practical profile

1. Introduction

The broad crested weir and weir with practical profile are widely used as a flow measurement structures in open channels. This type of weirs is easy to be constructed and installed. The flow on the weir with practical profile and broad crested weir of

sharp corners provides a classic example of flow separation. The simple geometry and the easily attainable two- dimensionally predestinates the weir geometry to study separation phenomena and dynamics of particles of different sizes in a broad crested weir of sharp corners flow. The characteristics of flow over

weir with practical profile and broad crested weirs have been extensively studied by old and recent investigations, while for the local integral flow quantities, i.e. the mean and turbulent velocity data are mostly lacking. The information regarding the turbulence characteristics in the weir with practical profile and broad crested weirs is somewhat scanty. Therefore, precise and accurate measurements of the mean and fluctuating flow quantities are carried out to study the depthwise variation of the turbulence intensities, and streamwise and vertical mean velocity distributions over the weirs. Particle transport and deposition in turbulent flows over the plate and turbulent jet has been investigated by Farmer [1], Simpson [2], and Popper [4]. Compared to the great number of experimental studies in particle laden channel flows, detailed experimental investigations of the particle size resolved dispersion in separated weir flows are rare. This holds specially for the technically most relevant particle diameter range of 10-100 μm . The dispersion of particles in a separated backward - facing step flow, have been reported by Ruck [5-7]. Experimental investigation on the turbulence in open channel flows using Laser Doppler Velocimetry, was reported by several investigators Ead [8], Nezu [9], Song [10], Shewey [11], Kironoto [12] and Attia [13]. Mcleland [14], Papanicolaou [15, 16] and Sukhodolov [17] investigated the turbulence structures in rough open channel flow. To measure particle velocities, Laser-Doppler Anemometry (LDA) [18, 19] is an advantageous measuring method because the velocity of the individual particles suspended in the flow can be measured directly.

Normal LDA applications infer the velocity information of a continuous fluid phase from the velocity data of small suspended particles. This can be done with a sufficient accuracy, as long as the particles are very small and ideally follow the flow fluctuations. The investigations in this paper describe the dynamics of particles of different sizes in the weir with practical profile and broad crested weir of sharp corners flow. The particle diameters under investigation were 10, 15, 25, 50, 75 and 100 μm . It seemed reasonable to

carry out experiments with a broad crested weir of sharp corners and weir with practical profile, which represents the most commonly investigated and understood flow separation regime. The experiments were carried out for turbulent flow conditions.

2. Experimental setup and test procedure

The measurements were carried out in a horizontal rectangular open channel that is 9800mm long, 100mm width and 500mm height with glass wall 6 mm thick and a steel plate bed. The flume and LDA system available at the Water Tunnel Laboratory at the Indian Institute of Technology, Bombay, India. Fig. 1 shows a layout of the test facility. The water is supplied from a sump to the inlet tank to the flume at a desired discharge that is continuously monitored with an on-line orifice meter. The flume side walls are made up of 6 mm thick glass sheets. A tail vertical gate was provided at the down stream end of the flume to maintain a required water depth of channel flow. The water was finally collected in a sump placed in the basement from where it was pumped back to the constant overhead tank by a 16 HP pump. The broad crested weir of sharp corners and weir with practical profile, were fabricated from transparent sheets.

With reference to the origin fixed at the channel bed along the centerline and in the starting of the weir, transverse of measuring volume was run to obtain the profiles of both the mean and fluctuating flow quantities (the mean velocity components and the turbulence intensities). The measuring points were closely spaced in the region of high velocity gradient. All the measurements were made for maximum discharge rate of 44 s^{-1} at a free stream water depth of $y_0 = 330$ mm. This gave Reynolds number based on the free stream velocity 5×10^4 which ensured the turbulent flow for all the test conditions. Froude number of the free stream $F_r = 0.248$, ensured the free stream flow to be subcritical. To obtain the vertical profiles of the mean and fluctuating quantities, the measurements were conducted in the vertical plane along the centerline at different location behind the weirs. In the vertical direction along

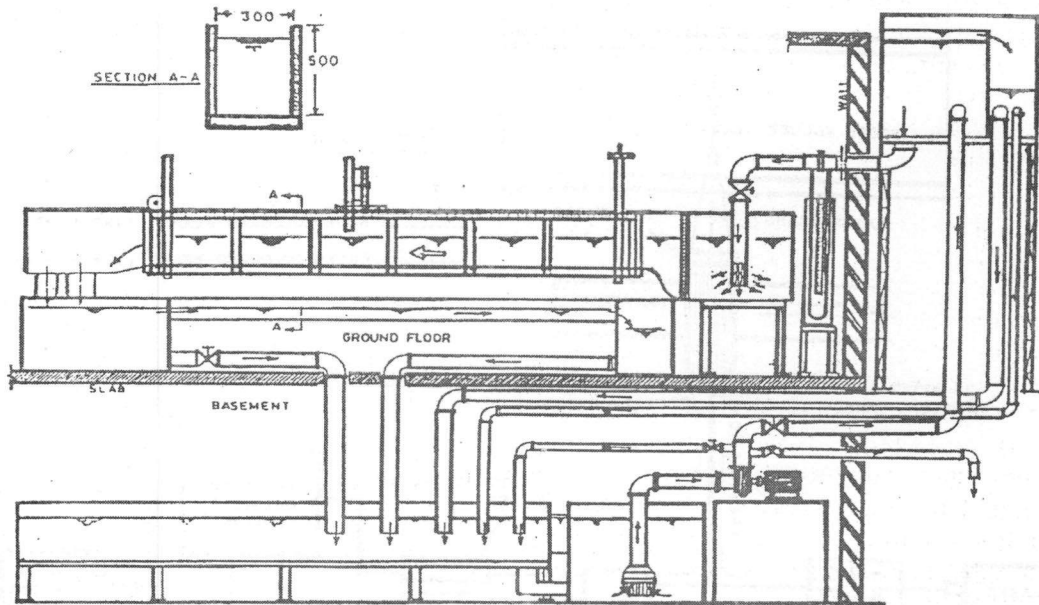


Fig. 1. Schematic of test facility.

the depth at the different cross sections, 30 measurements at 5 mm intervals up to 65 mm from the bed boundary and 15 mm for the rest were taken. The height [H] of the weirs were kept constant at 120 mm.

3. Instrumentation

The experimental data were collected using a DANTEC two color back- scatter LDA system, consisting of a 5 Watt- ion laser with two laser beams one blue [488nm] and one green [514.5nm], a fiber- optic measuring probe in back- scatter mode. Two Burst Spectrum Analyzers (BSA) were used to evaluate the Doppler frequencies, and subsequent computer analysis consisted of velocity bias averaging and outlier rejection. Fig. 2 shows a block diagram of the two component LDA set up used for the measurements. On a traverse bench, the measuring probe [laser beams or measuring volume] was focused on measuring a point from one side of the channel glass wall through an optical lens. The number of samples taken at every point was 1000 bursts. This corresponds to a simple averaging time of about 100 seconds. The data rate was about 10-20 Hz. Before acquiring the data, the LDA signal was checked for its regular Doppler burst that correspond to a particle passing

through the measuring volume. The measurements were taken at different positions downstream of the weir with practical profile and broad crested weir of sharp corners. Fig. 3 shows the location of the measuring sections [x/H] in the downstream of the weir.

4. Results and discussion

Measurements were made for various flow conditions. However, only representative results are presented here. The turbulence intensity components are non-dimensionalized by the streamwise mean free stream velocity in x-direction U_0 . The water depth is non-dimensionalized by the free stream water depth y_0 . Turbulence at the wall is construed to be turbulence at a very location from the wall of the order of 3 mm as observed in LDA experimentation and not at the wall it self perse. It may be mentioned here that the minimum distance away from the boundary at the turbulence and velocity measurements commenced was 5 mm. At the boundary, velocity and turbulence are zero. The two dimensions of the free stream flow was examined by measuring the spanwise distribution of the streamwise velocity components.

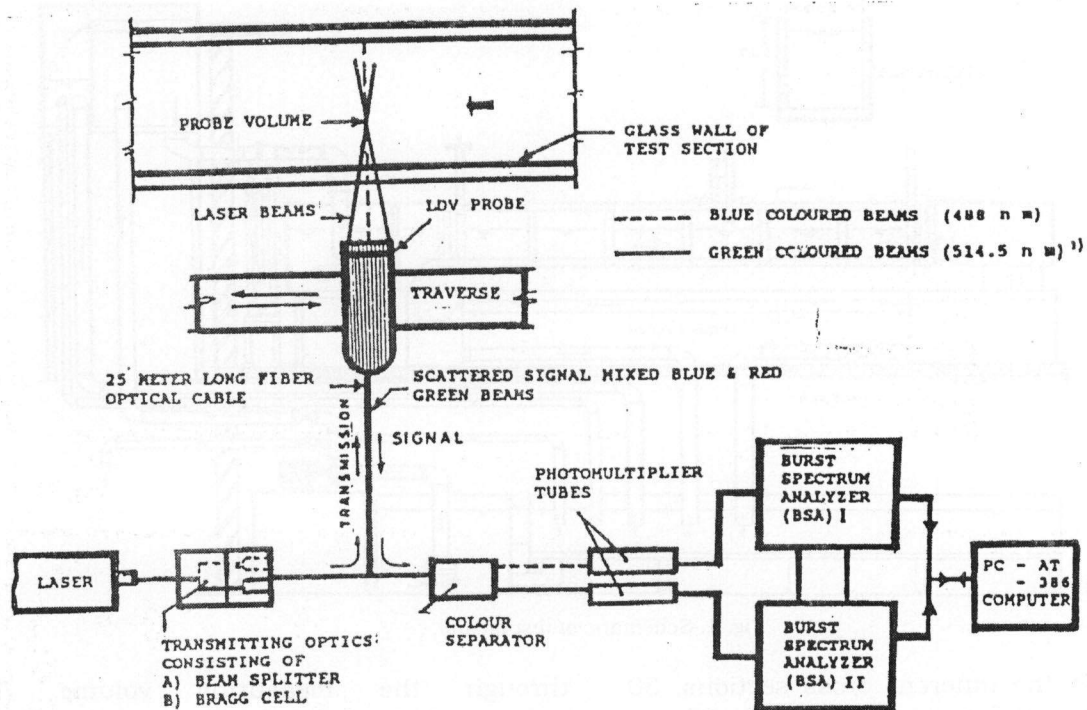


Fig. 2. Block diagram of the Laser Doppler Velocimetry (LDV).

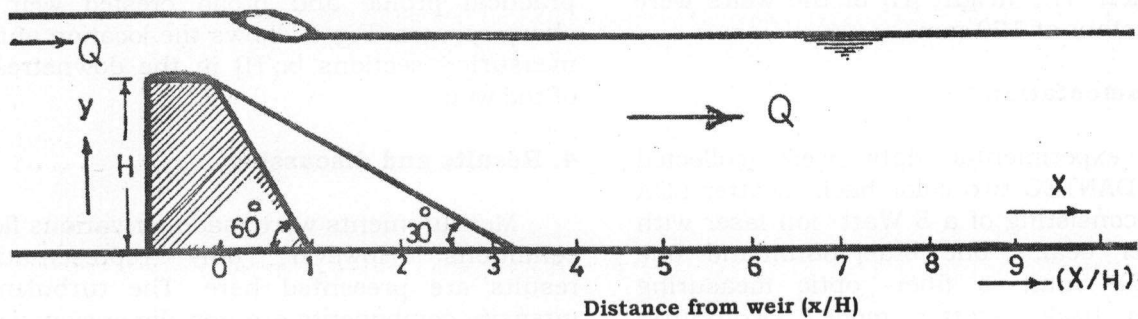


Fig. 3. Definition sketch of the weir with practical profile.

The following results represent time-averaged flow velocities and turbulence data. It should be remarked that the actual local mean data are ensemble averaged quantities, which rely on 1000 single LDA bursts. As mentioned before, the signal processing was performed by a transient recorder-microcomputer combination. The processable data rate was about 10 readings per second which is rather low predominantly caused by the data handing between recorder and computer.

Fig. 4 shows two typical series profiles of measured streamwise mean velocity

distribution \bar{u} / U_0 after the broadened crested weir of sharp corners for the suspended particles of 10 and 50 μm diameter for a maximum discharge of 44 $1/\text{s}^{-1}$, at different locations. It can be inferred that the 50 mm particles show smaller recirculating velocities than 10 μm particles. Furthermore, a smaller recirculation zone would be inferred from the velocity profile of the larger particles. As a trend, all the experiments deliver higher positive values for bigger particles in all the cross sections under investigation. The streamwise mean velocity \bar{u} / U_0 varies considerably according to the flow conditions.

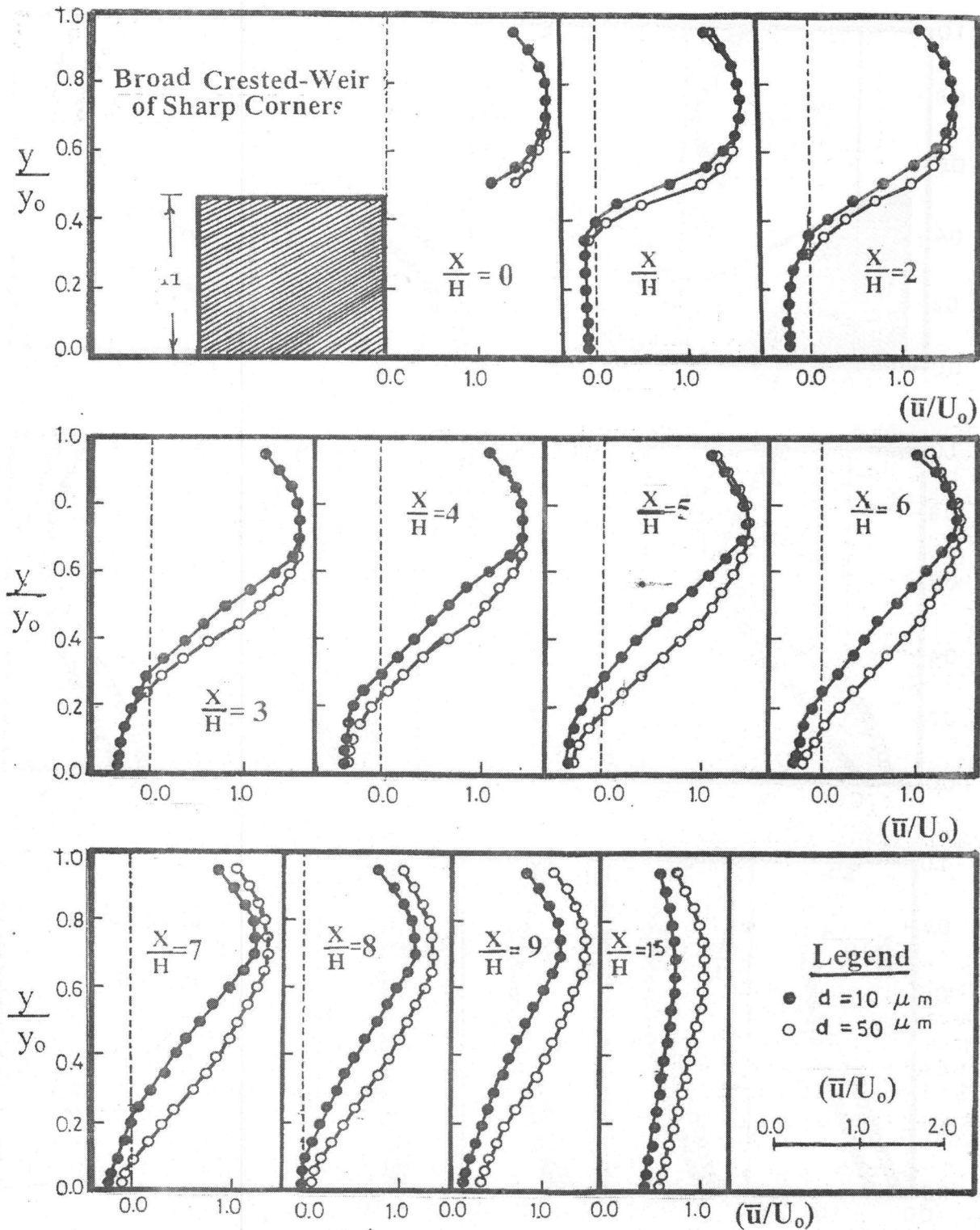


Fig. 4. Variation of streamwise mean velocity \bar{u}/U_0 with y/y_0 behind the broad crested-weir of sharp corners at different positions for $d = 10$ and $50 \mu m$ dia particles.

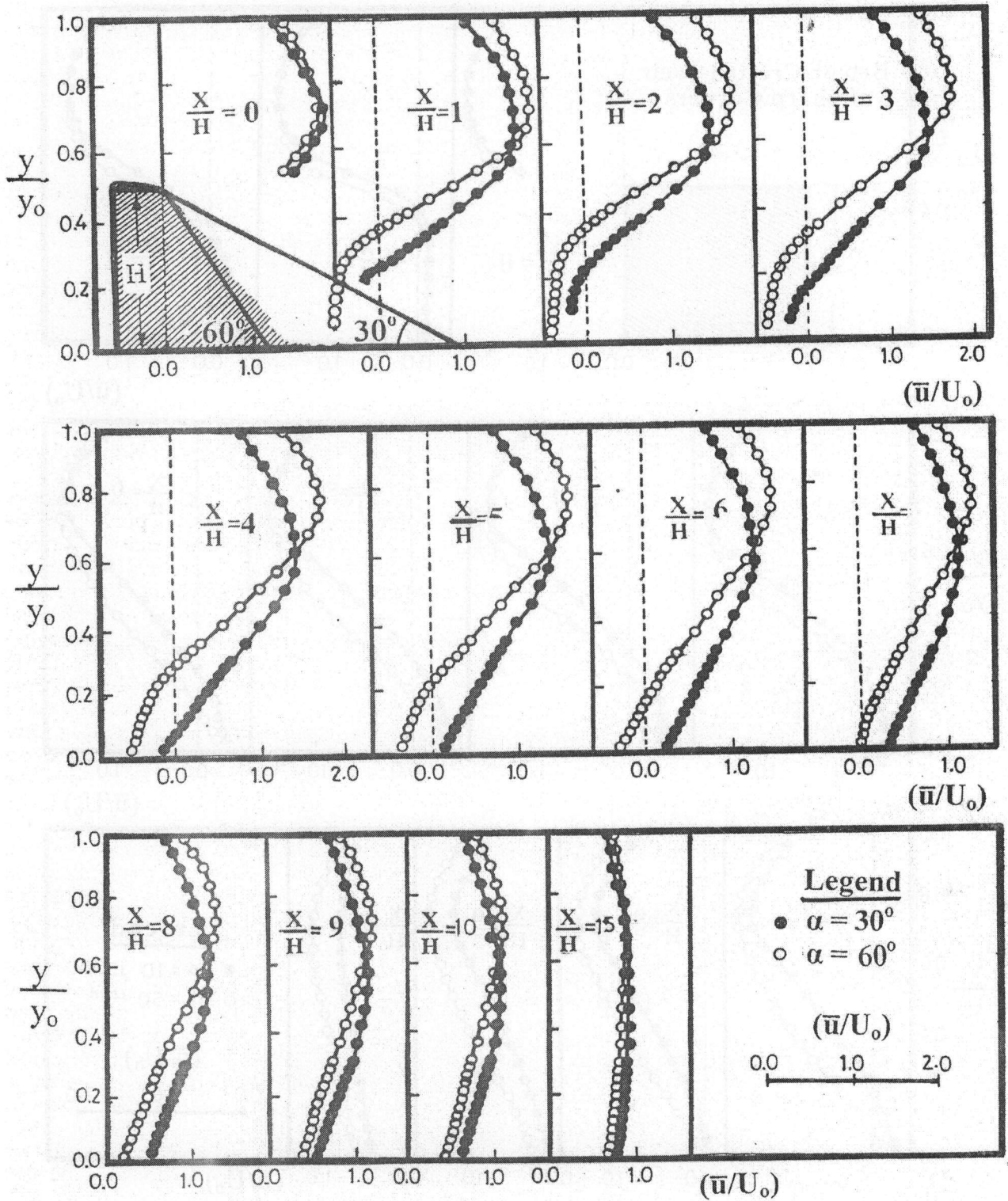


Fig. 5. Variation of streamwise mean velocity \bar{u}/U_0 with y/y_0 behind the weir with practical profile at different positions for $\alpha = 30^\circ$ and 60° .

Near the corner locations of the weir, reversal flow could be observed in the expansion zone behind the weir as shown in fig. 5 at $x/H=1.2.3.4.5.6$ and 7. This can also be seen in the shape of the velocity profile, and was observed visually during the experiment. Also, fig. 5 depicts the profiles of streamwise mean velocity distribution \bar{u}/U_0 behind the weir with practical profile with downstream angles of 30° and 60° for a maximum discharge of 44 l/s^{-1} , at different positions downstream of the weir with practical profile. The streamwise velocity \bar{u}/U_0 varies considerably according to the weir with practical profile angle (α). The reversal flow could be observed behind the weir with practical profile as shown in fig. 5 at $x/H=1.2.3.4.5$ and 6. However, the gradual weir with practical profile of 60° drastically changes the profile shape. Velocity profiles in gradual weir with practical profile of 30° show greater uniformity of streamwise mean velocity distribution along the channel depth. In broad crested weir, the velocity distribution along the depth shows a curvilinear nature, with greater magnitude carried over larger distance downstream the weir. In the weir with practical profile, not only reduces the velocity acceleration, but also influences the viscous effects close to the channel bed since wall shear stress is reduced from the velocity at the closest point to the bed. This indicates that the weir with practical profile has reduced velocity profiles compared to broad crested weir of sharp corners indicating better efficiency of smoother transition in energy reduction, with the same length. It can be observed that, in the weir with practical profile, the maximum negative (counter streamwise) velocities in the recirculation zone are reduced. In the external flow over the separation bubble, the maximum positive velocities are reduced as well as for flattened down stream side of the weir with practical profile up to position $x/H=5$. For flatter weir with practical profile the location of the maximum mean velocity U^+_{max} moves towards the middle of the channel behind the weir with practical profile edge.

Figs. 6 and 7 depict the maximum positive streamwise u^+_{max}/U_0 and maximum negative

counter streamwise velocity u^-_{max}/U_0 for the velocity profile along the longitudinal direction normalized with U_0 as a function of the channel length $[x/H]$ in the downstream zone of the broad crested weir of particles of different sizes. The aforementioned particle dynamics are reflected well in these graphs. It can be inferred that up to position $x/H \approx 3$ no significant changes between the particle velocities in the streamwise recirculation direction can be observed. The differences in particle velocity data begin to grow behind $x/H \approx 3$. The position of the maximum negative velocity in the separation zone is shifted to slightly smaller values of x/H with increasing particle size, but still remains around $x/H=4$. As shown, the particle velocity data of different particle classes deviate from each other. If the particle information is used to describe the continuous phase flow field, different velocity profiles will result.

Further information about the velocity field of the weir with practical profile can be derived from the maximum positive velocity data of the external flow and the maximum negative velocity data of the recirculation zone as a function of the streamwise channel coordinate. Fig. 8 shows the maximum positive velocity u^+_{max}/U_0 normalized with U_0 as a function of the channel length x/H for different weir with practical profile angles of 30° and 60° . For the fluid mass coming from the inlet, the dividing streamline represents an effective boundary limiting the effective channel cross section. It is noticed that the velocity profile occupies the lower position for the 30° weir with practical profile flow and the higher for the 60° weir with practical profile flow. The velocity decreases steadily for the edge location along the downstream direction in all cases. The maximum negative streamwise velocity u^-_{max}/U_0 along the longitudinal direction normalized with U_0 as a function of the channel length x/H in the downstream zone of the weir with practical profile is shown in fig. 9. For different weir with practical profile angles, the maximum of u^-_{max}/U_0 is registered for the weir with practical profile in the middle of the separation zone. for $\alpha=60^\circ$ the peak of maximum counter streamwise velocity is up to 5% higher than for the 30° weir with practical profile flow.

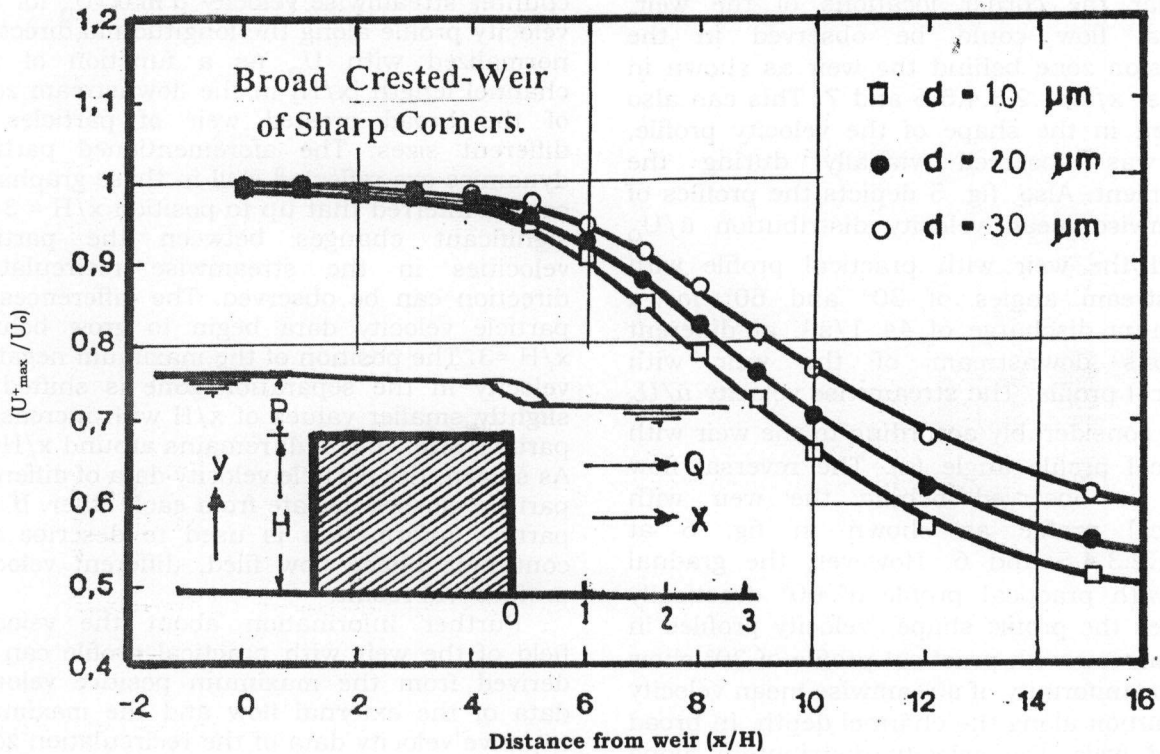


Fig. 6. Maximum positive velocity u^+_{max} (normal with u_0) in the streamwise portion of the velocity profile of particles of different sizes.

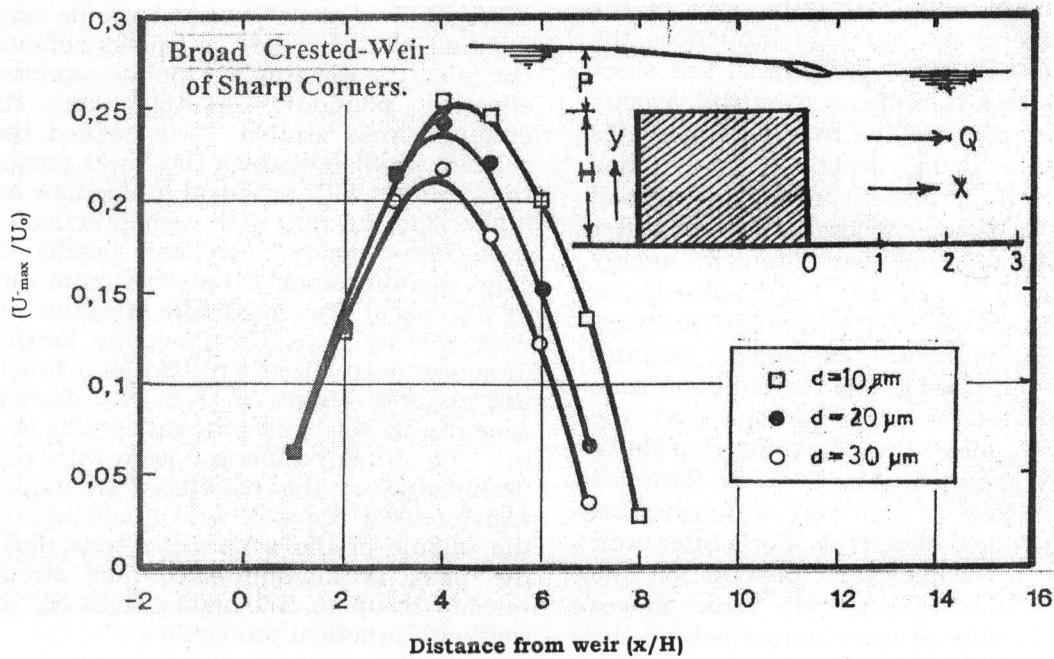


Fig. 7. Maximum negative velocity u^-_{max} (normal with u_0) in the streamwise portion of the velocity profile of particles of different sizes.

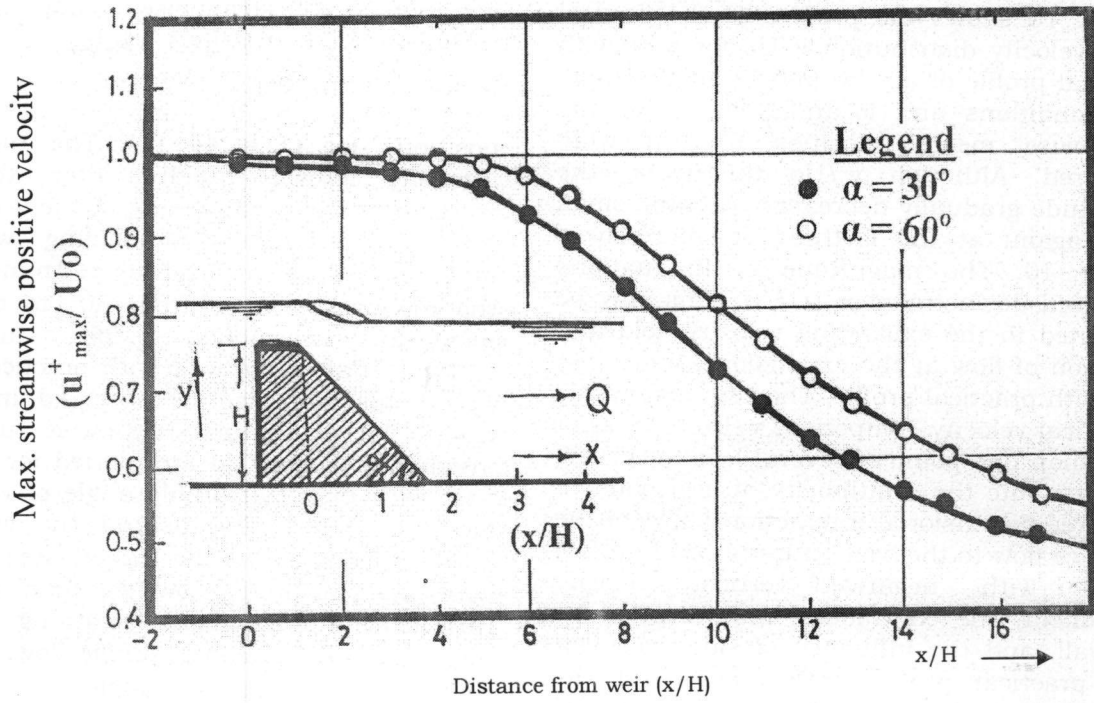


Fig. 8. Variation of maximum streamwise positive velocity u_{max}^+ / U_0 along the centerline behind the weir with practical profile for different angles.

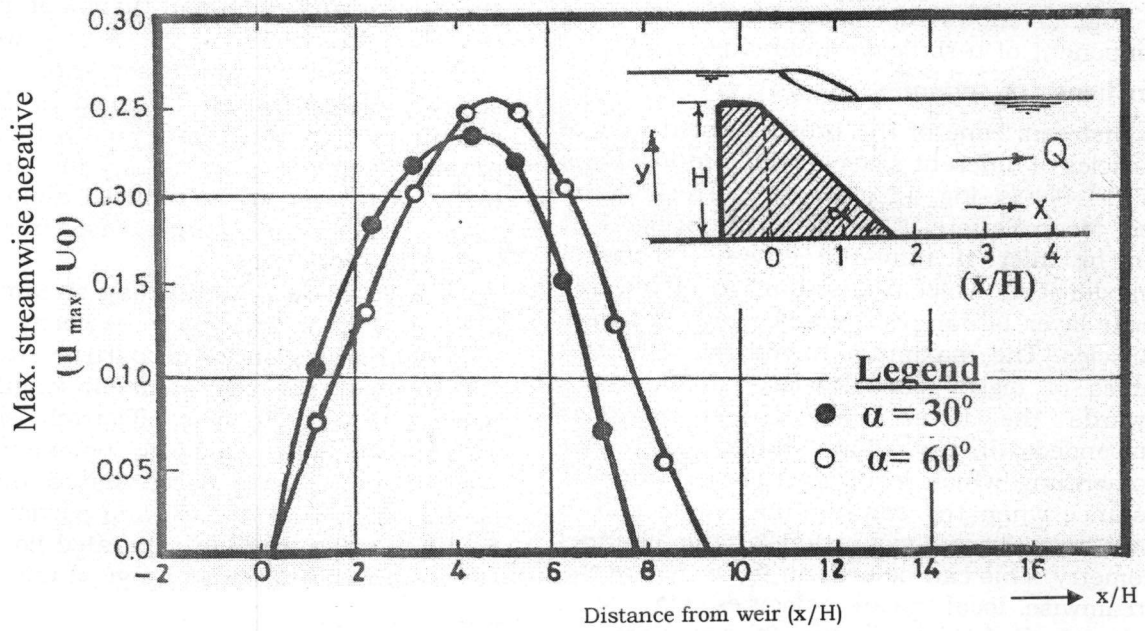


Fig. 9. Variation of maximum streamwise negative velocity u_{max}^- / U_0 along the centerline downstream the weir with practical profile for different angles.

Fig. 10 shows the profiles of the vertical mean velocity distribution v/U_0 for weir with practical profile of $\alpha = 30$ and 60 at the same flow conditions and locations at which the streamwise mean velocities \bar{u}/U_0 were measured. Although v/U_0 fluctuates, the magnitude gradually decreases reaching small value again at the farthest downstream of $x/H = 10$. The magnitude of fluctuations decreased downstream $x/H > 6$. This may be attributed to the expanding velocity field and diversion of flow at the expansion zone of the weir with practical profile. The zero magnitude of vertical velocity component v/U_0 , occurs at more than one point at several locations. One may attribute the multiplicity of null point to the three dimensional interaction between the entrance flow to the weir with practical profile, almost with negative vertical velocity component, the contracting flow diverted by the wall, and the influence of side wall weir with practical profile itself along with the horizontal bed impeding the downward component of velocity. This complex interaction would influence the flow pattern giving rise to multiplicity of null point.

Fig. 11 shows the variation of streamwise component of turbulence intensities u'/U_0 as functions of channel depth y/y_0 in the downstream zone of the broad crested weir of particles of different sizes at different locations for $Q = 44$ l/s. Fig. 11 gives the corresponding Root Mean Square [RMS] velocities of fig. 4. It can be inferred that the cross - sectional bimodal RMS, velocity distribution in the free shear layer is damped significantly for bigger particles. The maximum turbulence intensity values of bigger particles are shifted more towards the lower wall. Bigger particles suspended in a flow have a higher momentum, which leads to a longer stopping distance when the continuous flow is shown down, e.g. by an expansion of the channel geometry. This can be seen in fig. 6, where the streamwise local mean velocities stay at a higher level longer for the $30 \mu\text{m}$ particles than for the smaller ones. Fig. 13 depicts the

variation of streamwise component of turbulence fluctuations u'/U_0 in the downstream zone of the weir with practical profile for $\alpha = 30^\circ$ and 60° at different positions for $Q = 44$ l/s. The turbulence intensity grows rapidly after the flow separation and is spreading in the y -direction further downstream, coinciding with the developing of a new shear layer. An increase of the inclination angle from 30° to 60° does increase enormously the turbulence intensities after the weir with practical profile edge. This can also be observed in fig. 14 where the maximum streamwise turbulence intensities u'_{max}/U_0 are plotted for different weir with practical profile angle of variations along the centerline behind the weir with practical profile. For the investigated 30° weir with practical profile flow, the development of turbulence intensity is not as strong as for the 60° - weir with practical profile flow. For weir with practical profile angle $\alpha = 30^\circ$, the turbulent structure of the external flow at $y/y_0 \geq 0.6$ shows only small deviations. The slight increase of turbulence intensity in the shear layer and the small turbulent growth in the y - direction for the 30° - weir with practical profile flow does not influence strongly the turbulent flow field in the upper channel section. After 15 weir with practical profile heights $x/H = 15$, the maximum turbulence intensity is reduced almost to the same level of the streamwise free stream turbulence intensity.

Fig. 12 shows the dividing streamline and line of streamwise zero velocity in the recirculation region for all particle size classes investigated. The reattachment length of the particle velocity field is effectively shortened with increasing particle diameter. The experiments show clearly that a distinction between flow velocity field and particle velocity field has to be made in separated flow regions even in the particle size range of micrometers.

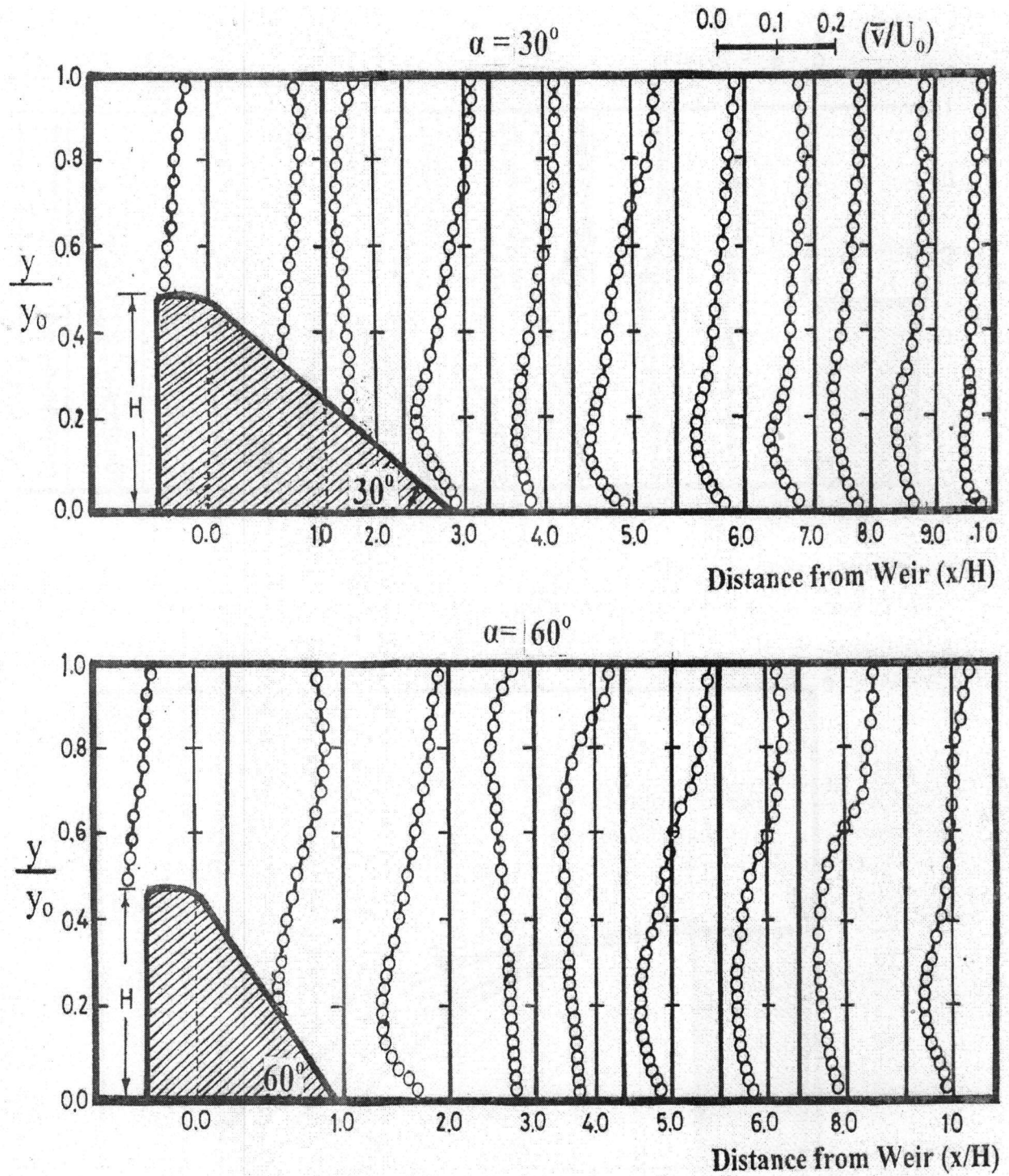


Fig. 10. Variation of vertical mean velocity \bar{u}/U_0 with y/y_0 downstream the weir with practical profile at different positions for $\alpha = 30^\circ$ and 60° .

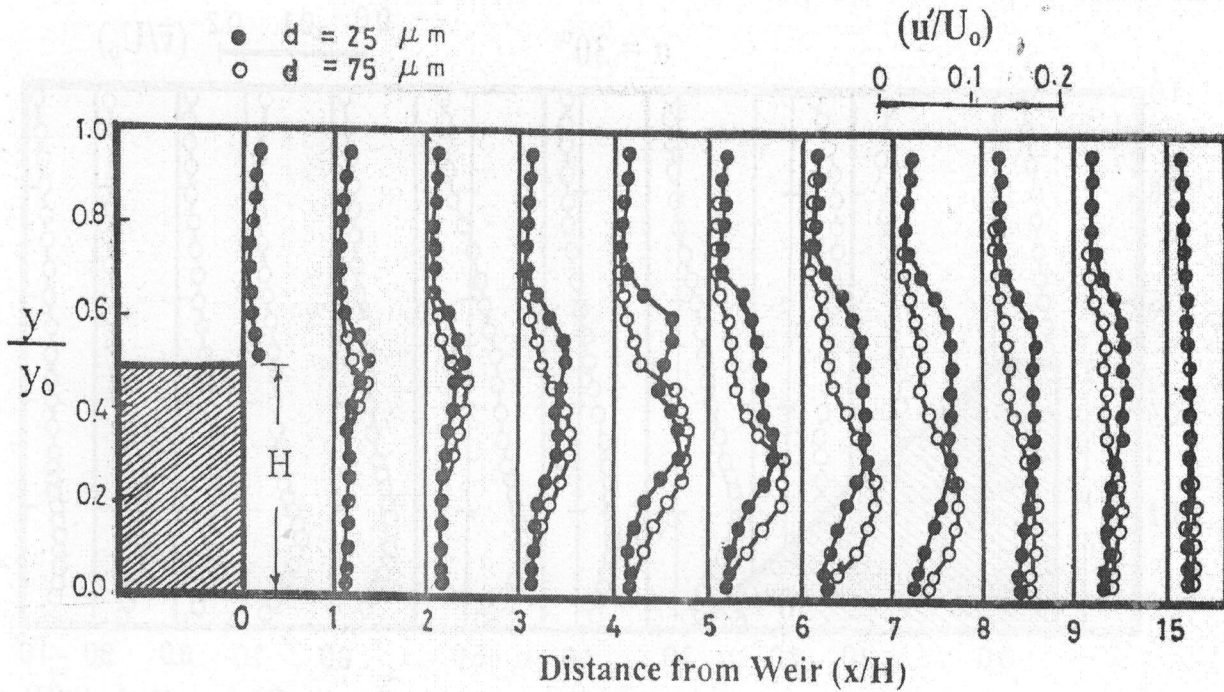


Fig. 11. Variation of vertical mean velocity (\bar{u}/U_0) with y/y_0 behind the broad crested weir of sharp corners for 1 and 70 μm dia particles.

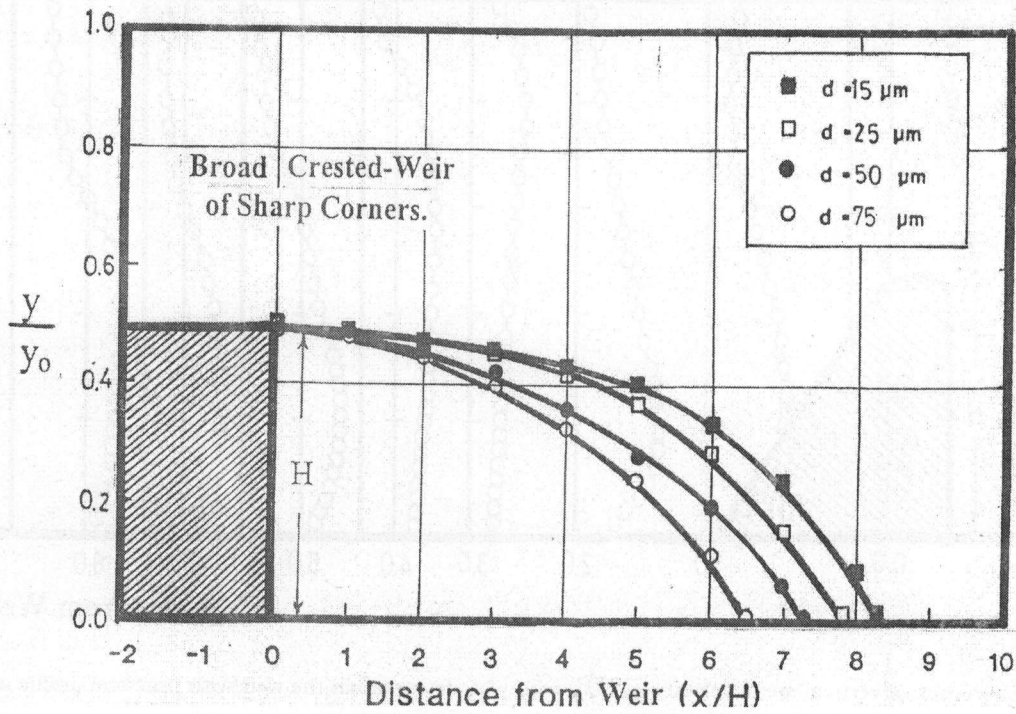


Fig. 12. Dividing streamline derived from velocities of particles of different sizes.

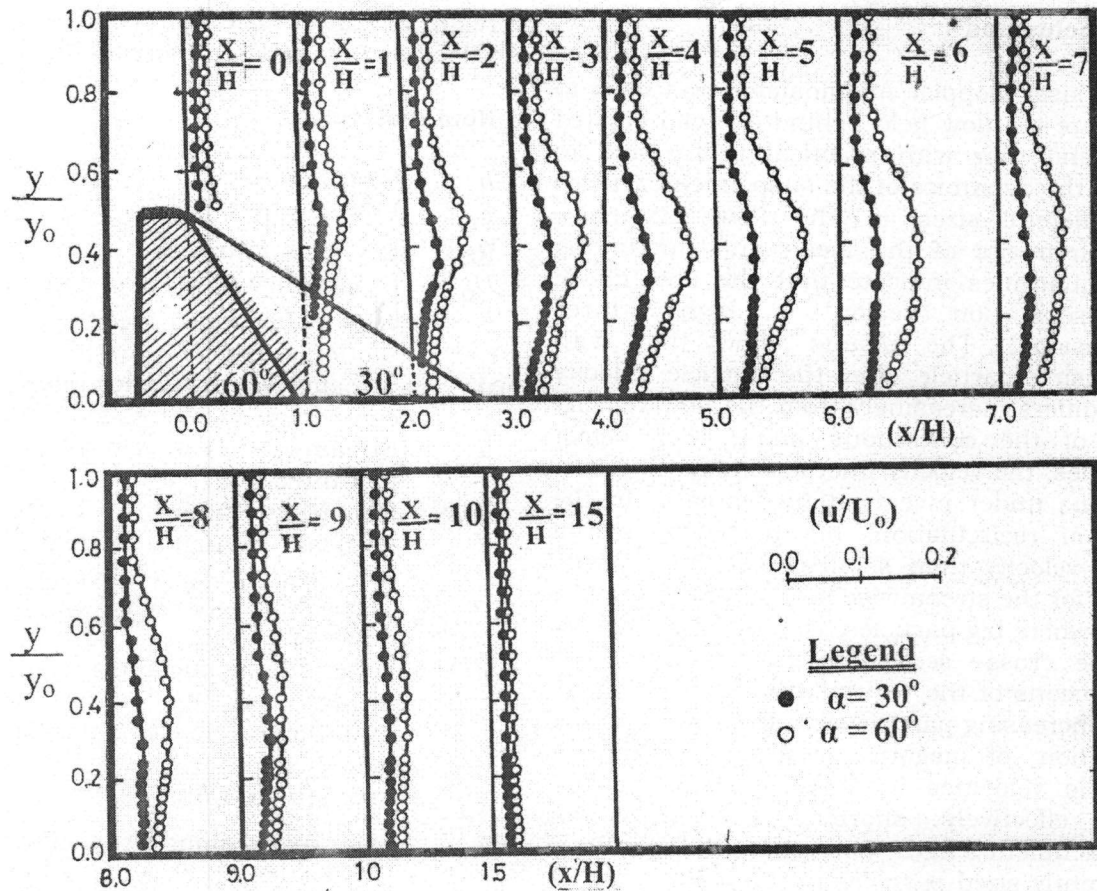


Fig. 13. Variation of vertical mean velocity (u'/U_0) with y/y_0 behind the weir with practical profile at different position for $\alpha = 30^\circ$ and 60° .

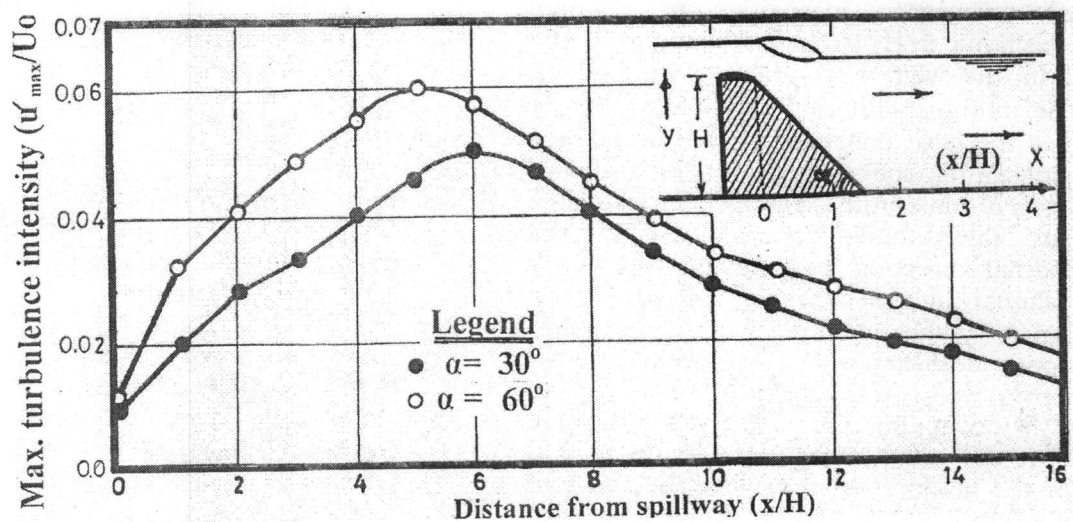


Fig. 14. Variation of maximum streamwise turbulence intensities (u_{max}'/U_0) along the centerline behind the weir with practical profile for $\alpha = 30^\circ$ and 60° .

5. Conclusions

A laser Doppler Anemometer was used to measure the flow field behind a broad crested weir and weir with practical profile and to study the dynamics of the suspended particles of different sizes in the flow. Extensive measurements of the mean and fluctuating flow quantities indicate that the flow inside the separation region is highly three dimensional. The results show that with increasing particle size, the particle velocity field differs increasingly from the flow velocity field of the continuous phase. For bigger particles, the velocity fluctuations in all cross-sections under investigation decrease. In the zone of recirculation, big particles have a lower velocity than small ones. The opposite holds for the streamwise portion of the velocity field, where big particles have a higher velocity in the cross-sections near the weir. The dimensions of the recirculation zone decrease with increasing particle size. This is due to the reduction of negative counter streamwise particle velocities in the separation region, with effectively shortens the measured reattachment length. Comparing the results of differently sized particles in the flow, it can be inferred that particle diffusion differs from the eddy diffusion even in the range of micron-sized particles. The results point out, that the highest turbulence intensities in channel cross sections $x/H < 10$ in both cases of the weirs. In the weir with practical profile, an increase in the inclination angle from 30° to 60° does increase enormously the turbulence intensities after the weir edge. The trend of variations of maximum streamwise turbulence intensity fluctuations \dot{u}_{max}/U_0 along the longitudinal direction behind the weirs, are quite similar in the cases of the weir, rises rapidly, to reach maxima with subsequent monotonous decrease along the distance away from the weir, the maximum values of \dot{u}_{max}/U_0 occur for the weir with practical profile at the range of x/H of 3.0 up to 6.3, and for the broad crested weir at the range of x/H of 4.0 to 7.5. The velocity profiles after the weir edge become more and more asymmetric and the velocity gradient in the shear layer is growing. In the weir with practical profile, it can be seen that steeper inclination angle

result in higher maximum counter streamwise velocities \dot{u}_{max}/U_0 in the recirculation.

Nomenclature

b	Channel width,
F_r	Froude number,
Re	Reynolds number,
U_0	Streamwise mean free stream, velocity (averaged over the cross section),
\dot{u}	Streamwise turbulence intensity, component in x-direction (RMS),
\bar{u}	Streamwise mean velocity, component in x-direction,
RMS	Root Mean Square,
V	Vertical turbulence intensity component in y-direction (RMS),
$-$	
$**$	Vertical mean velocity component in y-direction,
X	Longitudinal axis along channel length,
y	Transverse axis along channel height,
y_0	Free stream water depth,
z	Lateral axis along channel width,
g	Gravitation acceleration,
Q	Flow discharge,
w	Lateral turbulence intensity, component in z-direction (RMS)
α	Weir with practical profile angle,
H	Weir height, and
LDA	Laser Doppler Anemometry.

References

- [1] R. Farmer, P. Griffith and W.M. Rohsenow, "Liquid Droplet Deposition in Two-Phase Flow", J. of Heat Transfer, pp. 587-594 (1970).
- [2] H.C. Simpson and E.K. Brolls, "Droplet Deposition on a Flat Plate from an Air/Water Mist in Turbulent Flow Over the Plate", Symp. On Two Phase Flow Systems (A3), University of Strathclyde, Glasgow, 1 (1974).
- [3] G. Hetsroni and M. Sokolov, "Distribution of Mass, Velocity and Intensity of Turbulence in a Two-Phase Turbulent Jet", J. Applied Mech., pp. 315-327 (1971),

- [4] J. Popper, N. Abuaf and G. Hetsroni, "Velocity Measurements in a Two- Phase Turbulent Jet", *Int. J. Multiphase Flow*, pp. 1.715-726 (1974)
- [5] B. Ruck, F. Schmith and T. Loy, "Particle Dynamics in a Separated Step Flow", 3rd Int. Symp. On Application of Laser- Anemometry to Fluid Mechanics, Lissabon, Proc., Chapter 2.1 (1988).
- [6] B. Ruck and B., Makiolo, "The Dispersion of Particles in a Separated Backward- Facing Step Flow", Proc. Of IUTAM Symp. 20-24.8.90, la Jolla, California- USA (1990).
- [7] B. Ruck and B. Makiola, "Particle Dispersion in a Single- Sided Backward Facing Step Flow" *Int. Journal Multiphase flow*, Vol. 14 (0.6), pp.787-800 (1988).
- [8] S. Ead, N. Ragaratnam, C. Katopodis and F. Ade, "Turbulent Open Channel Flow in Circular Corrugated Culverts," *J. Hydraul. Eng.*, Vol. 126 (10), pp. 750-757 [2000].
- [9] I. Nezu and H. Nakagawa, "Turbulence in Open Channel Flows" A.A. Balkema, Rotterdam, the Netherlands (1993).
- [10] T. Song and Y. Chiew, "Turbulence Measurement in Non uniform Open Channel Flow Using Acoustic Doppler Velocimeter (ADV)", *J. Eng. Mech.* Vol. 127 (3), pp. 219- 231 (2000).
- [11] M.I.A. El- Shewey and S.G. Joshi, "A Study of Turbulence Characteristics in Open Channel Transitions as a Function of Froude and Reynolds Numbers using Laser Technique", *Adv Fluid Mech.*, Vol. 9, pp. 363-372 (1996).
- [12] B.A. Kironoto and W.H. Graf, "Turbulence Characteristics in Rough Uniform Open Channel Flow", *Proc., Inst. Civ. Eng., Waters Maritime Energy*. 98 (1994).
- [13] M.I. Attia, "Experimental Investigation of the Influence of Inclined Depression on the Turbulent Flows in Open Channel Using Laser Doppler Velocimetry (LDV), *J. Eng. Research, Faculty of Engg., Mataria., Egypt.* Vol.108, Dec. (2006).
- [14] S. Mcleland, P. Asworth, J. Best and J. Livesey, "Turbulence and Secondary Flow over Sediment Stripes in Weakly Bimodal Bed Material", *J. Secondary Flows*, Vol. 125 (5), pp. 463-473 (1999).
- [15] A. Papanicolaou, "The Role of Turbulence on the Initiation of Sediment Motion," PHD Dissertation Virginia Polytechnic Institute and State Univ., Blacksburg, Va (1997).
- [16] A. Papanicolaou, P. Diplas, C. Dancy and M. Balakrishnan, "Surface Roughness Effects in Near- Bed Turbulence: Implications to Sediment Entrainment", *J., Eng. Mech.*, Vol. 127 (3), pp. 211-218 (2001).
- [17] A. Sukhodolov, M. Thiele and H. Bungartz, "Turbulence Structure in a River Reach with Sand Beds", *Water Resour. Res.*, Vol. 34 (5), pp. 1317-1334 (1998).
- [18] B. Ruck, "Laser Doppler Anemometry-A Non- Intrusive Optical Measuring Technique for Fluid Velocity", *Particle Charact.* 4/87, pp. 26-37 (1987).
- [19] F. Durst, A. Melling and J.H. Whitelaw, "Pemometry", Academic Press, London (1976).

Received August 27, 2008
Accepted August 26, 2009

